

Experimental and theoretical studies of the reaction of atomic hydrogen with silane

A. Goumri, W.-J. Yuan, Luying Ding, Youchun Shi and Paul Marshall

Department of Chemistry, University of North Texas, P.O. Box 5068, Denton, TX 76203-5068, USA

Received 12 May 1993

The kinetics of the reaction $\text{H}(1^2\text{S}) + \text{SiH}_4$ have been measured from 290 to 660 K by the flash photolysis–resonance fluorescence technique. The results are summarized by $k = (1.78 \pm 0.11) \times 10^{-10} \exp[-(16.0 \pm 0.2) \text{ kJ mol}^{-1}/RT] \text{ cm}^3 \text{ s}^{-1}$ with a confidence interval of about $\pm 10\%$. The transition state for direct H-atom abstraction was investigated theoretically, at up to the GAUSSIAN 2 ab initio level. A transition state theory analysis of the abstraction channel gives excellent accord with the measurements, which suggests that $\text{H}_2 + \text{SiH}_3$ are the dominant products. An expression for the reverse reaction is given. An extrapolated k from 290 up to 2000 K, which includes a Wigner tunneling correction, is $k = 2.44 \times 10^{16} (T/\text{K})^{1.903} \exp(-1102 \text{ K}/T) \text{ cm}^3 \text{ s}^{-1}$.

1. Introduction

The gas-phase reaction of $\text{H}(1^2\text{S})$ with silane has one thermodynamically accessible product channel,



and is a critical step in many chemical vapor deposition (CVD) processes because of the important role of SiH_3 [1–4]. As may be seen from table 1, there is a spread of a factor of 40 between the lowest and highest determinations of the rate constant k at room

Table 1
Summary of rate constants measured for $\text{H} + \text{SiH}_4$ at room temperature

$k(298 \text{ K}) (10^{-13} \text{ cm}^3 \text{ s}^{-1})$	Ref.
≥ 4	[5,6]
>2.2	[7]
13 ± 4	[8]
26 ± 3	[9]
85 ± 43	[10]
$2.2 \pm 0.3 (4.4)^{\text{a}}$	[11]
$2.3 \pm 0.3 (4.6)^{\text{a}}$	[12]
4.4 ± 0.7	[13]
2.0 ± 0.1	[14]
2.2 ± 0.2	[15]
2.8 ± 0.3	this work

^a) Reevaluated in ref. [14], original value in parentheses.

temperature ^{#1} [7–15] and only one of the most recent studies, by Arthur et al. [14], investigated the temperature dependence of k . There has been a recent study of isotopic exchange between translationally hot H atoms and SiD_4 and SiH_3D [16], while two other studies have yielded Arrhenius parameters for isotopic variations of reaction (1) [17,18]. We note that Arthur et al. obtained a pre-exponential factor of about $2 \times 10^{-11} \text{ cm}^3 \text{ s}^{-1}$ for reaction (1), which is an order of magnitude smaller than found for H-atom reactions with the valence-isoelectronic first-row hydrides CH_4 , NH_3 and H_2O (see e.g. table 2 of ref. [19]). The first part of the present study is a reexamination of the temperature dependence of reaction (1) with a different technique over a wider range of temperature.

Several of the investigations summarized in table 1 also included semi-empirical BEBO analyses [20], some of which were found to be in accord with experiment and some not. These disagreements reflect (i) the difficulty of uniquely interpreting a k value measured at a single temperature in terms of two Arrhenius parameters, which cannot be separated, (ii) uncertainties in the BEBO input parameters, especially

^{#1} k was found to be “much greater” than the rate constant for $\text{H} + \text{C}_2\text{H}_4$ by Niki and Mains [5], which under their conditions was at least $4 \times 10^{-13} \text{ cm}^3 \text{ s}^{-1}$ [6].

the Si–H bond strength, and (iii) fundamental uncertainties in the BEBO method itself. There have also been two ab initio studies of a transition state (TS) for reaction (1) which yielded energies of the TS above the reactants at 0 K, E_0^* , in the range 32–45 kJ mol⁻¹ [21,22], but in neither case were the results related to kinetic measurements. Arthur et al. measured an activation energy $E_a \approx 12$ kJ mol⁻¹ [14]. While E_0^* is not identical to E_a , the difference between experiment and earlier ab initio theory corresponds to more than three orders of magnitude in the room-temperature rate constant. The second part of the present study is an ab initio investigation, at the highest level of theory to date, that resolves this discrepancy.

Two possible mechanisms for reaction (1) have been discussed, either direct H-atom abstraction or formation and dissociation of a bound SiH₅ intermediate. The idea of an SiH₅ intermediate was initially proposed by Glasgow et al. [23], and Nakamura et al. [24] suggested that they had formed this species in a frozen matrix, and detected it by ESR. However, previous ab initio analyses of possible SiH₅ structures have so far indicated that they are all saddle points in the potential energy surface (PES), rather than local minima, and also that they are endothermic with respect to H + SiH₄ [25–27]. The reactions of H with CH₄, NH₃ and H₂O are considered to proceed via direct abstraction, and good accord is found between kinetic analysis based on this assumption and experiment (see e.g. refs. [19,28–30]). Such analysis typically employs ab initio data combined with transition state theory (TST) and corrections for quantum-mechanical tunneling. Here we test whether a similar approach can explain the kinetics of reaction (1), and show that good agreement with the measured k is obtained.

2. Methodology

2.1. Experimental technique

Details of the apparatus and the application of the flash photolysis–resonance fluorescence technique have been described elsewhere [31,32]. Briefly, atomic hydrogen was generated by pulsed UV photolysis of ammonia using a small flash lamp. The H

atoms reacted with an excess of silane under pseudo-first-order conditions,

$$\frac{d[H]}{dt} = -k_{\text{ps1}}[H] \\ = -(k_1[\text{SiH}_4] + k_{\text{diff}})[H], \quad (2)$$

where k_{diff} represents the loss of H atoms from the reaction zone by diffusion and reaction with NH₃ [19,33]. All experiments were carried out in a large excess of argon bath gas (>99%) to ensure thermal equilibration. Relative [H] during the course of reaction (1–10 ms) was monitored by time-resolved atomic resonance fluorescence at $\lambda=121.6$ nm, H(2²P)→H(1²S). The vacuum UV fluorescence was excited by a microwave-powered discharge lamp through which flowed a dilution of 1% H₂ in Ar at about 100 Pa. Fluorescence was detected with a solar-blind photomultiplier tube optically coupled to the reactor via a magnesium fluoride window and a filter of 2.4 cm of dry flowing air. The narrow gap in the absorption spectrum of O₂ isolated the H-atom fluorescence from other vacuum UV radiation [34]. Pulse counting and signal averaging were employed, and the resulting plots of signal versus time (see fig. 1 inset) were analyzed as described earlier [31], to obtain k_{ps1} at a given pressure, temperature (T), [NH₃], [SiH₄], average residence time of the gas inside the reactor before photolysis (τ_{res}) and flash lamp energy (F). k was obtained from the slope of a linear plot of typically seven values of k_{ps1} versus [SiH₄],

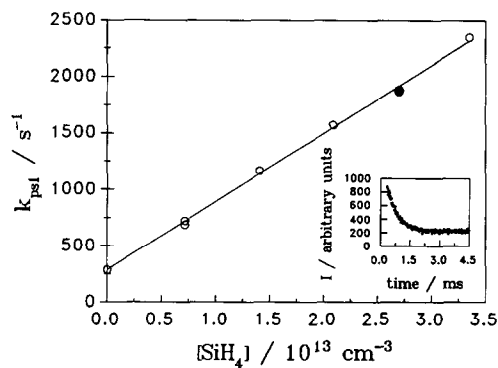


Fig. 1. Plot of pseudo-first-order decay coefficient for loss of H versus [SiH₄] obtained at 570 K and 46.7 mbar total pressure. The inset corresponds to the filled point and shows the decay of fluorescence plus a constant background of scattered light.

obtained with $[\text{SiH}_4]=0$ to $[\text{SiH}_4]_{\text{max}}$ and with all other parameters held constant, as shown in fig. 1. The uncertainty in individual k determinations, σ_k , was derived as outlined previously [31].

The temperature of the gas in the reaction zone was measured before and after each k determination with a type K thermocouple. Radiation errors were determined as described earlier [35]. The correction is zero at room temperature, reaches -10 K at about 520 K, and falls to zero at about 850 K. After this correction we allowed for a $\pm 2\%$ uncertainty in T to cover errors in the correction procedure and uncertainty in the thermocouple calibration. This propagates an additional 2% uncertainty into σ_k .

2.2. Ab initio calculations

The TS for direct H-atom abstraction from SiH_4 by H was investigated with ab initio methods [36], using the GAUSSIAN 90 program [37] on a VAX 6310 and a Solbourne 5E computer. The work of Gordon et al. [21] and Tachibana et al. [22] provided starting points for geometry optimization of SiH_4 and the SiH_3^\ddagger TS at two levels of spin-unrestricted theory, with a standard basis set that includes polarization functions on Si: HF/6-31G* (a Hartree-Fock calculation) and MP2/6-31G* (which includes a correction for electron correlation derived from second-order many-body perturbation theory applied to all electrons). The wavefunctions were verified to be HF stable [38] at each stationary point on the H + SiH_4 potential energy surface (PES), and vibrational frequencies were calculated to check that the geometries obtained for SiH_4 and SiH_3^\ddagger were a true minimum and a TS (with a single imaginary frequency), respectively. The HF frequencies were scaled by a standard factor of 0.893 [36], while the MP2 frequencies were scaled by a factor of 0.95. The reaction coordinate (RC) was followed forwards and backwards from the TS at the HF/3-21G(*) and MP2/6-31G* levels, using the algorithm of Gonzalez and Schlegel [39], to verify that the TS does indeed connect the reactants and products of reaction (1).

Next, energies were calculated at the HF/6-31G* and MP2/6-31G* geometries for the reactants and the TS with MP4/6-31G* theory. Finally, the GAUSSIAN 2 method of Pople and co-workers [40–42] was

applied to the TS to calculate a better estimate of its energy above the reactants at 0 K, E_δ^\ddagger . This approach approximates a complete QCISD(T)/6-311+G(3df, 2p) calculation by means of several additive corrections to the MP4/6-311G**||MP2/6-31G* energy. The G2 energy includes zero-point vibrational energy (ZPE) at the scaled HF/6-31G* level. We also tested the effect of including the scaled MP2/6-31G* ZPE instead, and denote the results as G2*. We define a spin-projected P-G2 energy as the G2 value plus a correction equal to the difference between the PMP4/6-311G** and MP4/6-311G** energies, where spin contamination has been projected out of the PMP4 energy using the algorithm of Schlegel [43].

Conventional TST was employed for the kinetic calculations, with the usual assumption of the separability of vibrational and rotational motions of the TS [20]

$$k_{\text{TST}} = \Gamma \frac{k_{\text{B}} T}{h} \frac{Q_{\text{SiH}_3^\ddagger}}{Q_{\text{H}} Q_{\text{SiH}_4}} \exp\left(-\frac{E_\delta^\ddagger}{RT}\right). \quad (3)$$

Γ represents a correction factor for quantum-mechanical tunneling and is ≥ 1 . Three models were considered: (A) no tunneling ($\Gamma=1$), (B) Wigner tunneling [44] based on the conjugate of the ab initio complex frequency for motion along the RC, ν^* , calculated at the MP2/6-31G* level,

$$\Gamma = 1 + \frac{1}{24} \left(\frac{h\nu^*}{k_{\text{B}} T}\right)^2, \quad (4)$$

and (C) Wigner tunneling based on a value of ν^* derived from fitting to the RC at the G2 level. MP2/6-31G* structural and vibrational data were used to calculate the partition functions Q , and the electronic partition function of the TS was assumed to be 2.

3. Results and discussion

3.1. Experimental results

Twenty-three determinations of k between 290 and 660 K are summarized in table 2. The absence of a consistent variation of k with the flash lamp energy (F) and $[\text{NH}_3]$, which were changed by factors 2 and 3, respectively, indicates that secondary chemistry of H with photolysis or reaction products was insignifi-

Table 2
Summary of kinetic data for H + SiH₄

<i>T</i> (K)	<i>P</i> (mbar)	τ_{res} (s)	<i>F</i> (J)	[NH ₃] (10 ¹⁵ cm ⁻³)	[SiH ₄] _{max} (10 ¹⁴ cm ⁻³)	<i>k</i> ± σ_k (10 ⁻¹² cm ³ s ⁻¹)
290	42.7	0.7	4.05	0.84	7.92	0.26 ± 0.06
290	42.7	0.7	4.05	1.39	8.03	0.27 ± 0.04
329	45.3	0.9	4.05	2.57	11.1	0.55 ± 0.06
330	43.1	0.8	5.00	2.10	12.9	0.60 ± 0.01
330	43.1	0.8	2.45	2.10	12.9	0.55 ± 0.01
379	43.7	0.6	2.45	1.57	4.32	0.99 ± 0.03
379	43.7	0.6	5.00	1.57	4.32	1.06 ± 0.03
382	42.5	1.1	2.45	3.06	2.80	1.11 ± 0.09
382	42.5	1.1	5.00	3.06	2.80	1.17 ± 0.17
449	43.9	1.0	2.45	1.48	4.83	2.30 ± 0.06
449	43.9	1.0	5.00	1.48	4.83	2.44 ± 0.05
449	59.7	1.4	4.05	2.02	5.14	2.44 ± 0.06
496	40.9	0.4	5.00	1.12	1.57	3.97 ± 0.13
496	40.9	0.4	2.45	1.12	2.07	3.99 ± 0.16
570	46.7	0.8	4.05	1.95	3.35	6.05 ± 0.12
570	46.7	0.8	4.05	0.98	3.52	5.81 ± 0.12
570	46.7	0.8	5.00	1.95	3.36	6.09 ± 0.12
570	46.7	0.8	2.45	1.95	3.36	5.76 ± 0.12
600	42.7	0.3	4.05	0.97	1.34	6.82 ± 0.14
600	41.6	0.7	4.05	1.05	2.50	6.85 ± 0.33
658	71.1	1.1	4.05	3.28	1.57	9.73 ± 0.43
658	70.3	1.0	4.05	3.25	1.28	10.35 ± 0.21
658	69.9	0.5	4.05	1.66	1.29	10.51 ± 0.21

cant. The lack of variation of *k* with the residence time of the gas mixtures inside the heated reactor before photolysis (τ_{res}), which was changed by a factor of 5, shows that thermal decomposition of NH₃ and SiH₄ was negligible and that the gases were well mixed. The *k* data are plotted in Arrhenius form on fig. 2. A weighted linear fit [45], that takes account of the un-

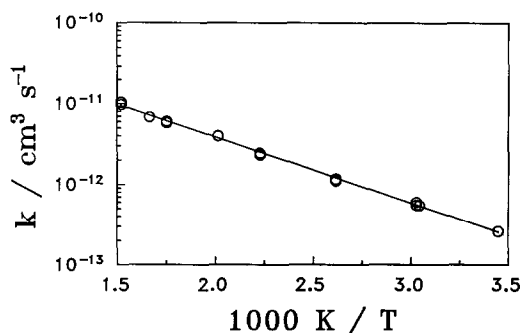


Fig. 2. Arrhenius plot of 23 measurements on the H + SiH₄ reaction.

certainties in *k* and *T*, to the form $A \exp(-E_a/RT)$ yields

$$k = (1.78 \pm 0.11) \times 10^{-10} \times \exp[-(16.0 \pm 0.2) \text{ kJ mol}^{-1}/RT] \text{ cm}^3 \text{ s}^{-1}. \quad (5)$$

The quoted errors represent $\pm 1\sigma$ in the Arrhenius parameters. These errors, combined with the covariance [46] yield statistical errors of $\sigma \approx 2\text{--}5\%$ over the temperature range. Allowance of $\pm 5\%$ for possible but unrecognized systematic errors leads to a 95% confidence interval for *k* of about $\pm 10\%$ over the experimental range.

Eq. (5) implies $k(298 \text{ K}) = (2.8 \pm 0.3) \times 10^{-13} \text{ cm}^3 \text{ s}^{-1}$, which is in reasonable accord with the two most recent room-temperature determinations, by Arthur et al. [14] and Koshi et al. [15] (see table 1). The earlier measurements in table 1 have already been critiqued by Arthur et al. [14], who revised the analysis in two cases [11,12]. Only the experiments of Arthur et al. [14] permit comparison with the pres-

ent work at higher temperatures. Their result for 290–490 K of

$$k = (2.3 \pm 0.3) \times 10^{-11} \times \exp(-11.6 \pm 0.3 \text{ kJ mol}^{-1}/RT) \text{ cm}^3 \text{ s}^{-1} \quad (6)$$

has markedly different Arrhenius parameters from eq. (5), although the k values themselves are in closer accord (see fig. 3). At 298 K the k values agree within about 25%, while at 490 K eq. (6) yields a k about one third of that from eq. (5), a significant deviation. Coltrin et al. [47] have recommended

$$k = 1.73 \times 10^{-10} \times \exp(-10.5 \text{ kJ mol}^{-1}/RT) \text{ cm}^3 \text{ s}^{-1} \quad (7)$$

for modeling CVD. Their assumed A factor is now verified experimentally, but their assumed E_a is too small, so that their k is overestimated by up to an order of magnitude at room temperature (see fig. 3). That CVD model may therefore require revision.

The fit of eq. (5) was combined with the equilibrium constant for reaction (1), calculated from ΔG_f^\ddagger

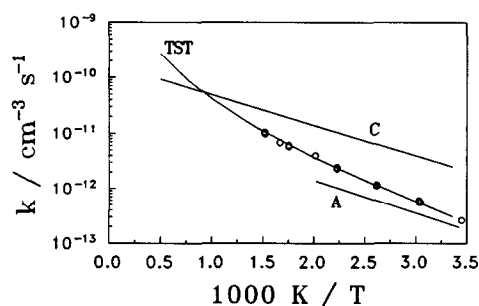


Fig. 3. Arrhenius plot showing measured k values (\circ); transition state theory fit (model C, see text) (TST); fit of Arthur et al. [14] (A); recommendation of Coltrin et al. [47] (C).

data for H, SiH₄, H₂ [48] and SiH₃ [49], to obtain the following expression for the rate constant k_{-1} for the reverse reaction over $T = 290$ –660 K:

$$k_{-1} = 5.1 \times 10^{-12} \times \exp(-67.4 \text{ kJ mol}^{-1}/RT) \text{ cm}^3 \text{ s}^{-1}, \quad (8)$$

with 95% error limits of about a factor of 3, mainly arising from uncertainty in $\Delta H_f^\ddagger(\text{SiH}_3)$.

3.2. Theoretical analysis

The ab initio geometries for stationary points on the PES are given in table 3. The results are of course identical with previous equivalent calculations where they exist [22,36]. The HF results for the TS agree quite closely with the HF/3-21G geometry of Gordon et al. [21]. The MP2 calculations on the TS, by comparison with the HF data, suggest that inclusion of electron correlation yields a slightly looser TS, with a longer H–H partial bond and a shorter Si–H partial bond. Typically MP2 theory leads to longer bonds than HF theory [36], and this can be seen in table 3. For H₂ and SiH₄ the MP2 results are closer to the experimental values [36] and we therefore employ results from MP2 theory in the kinetic calculations below. Vibrational frequencies at stationary points in the H + SiH₄ PES are summarized in table 4. Values for SiH₄ and SiH₃ have been compared with experiment elsewhere [50]. For H₂ the error at the scaled HF level is only 6 cm⁻¹, but is 150 cm⁻¹ at the MP2 level.

A search for possible bound SiH₅ species at the MP2/6-31G* level led only to a loose adduct between H + SiH₄, with a very long Si–H distance of about 4.1 Å. All frequencies were real, but energy calculations at up to the G2 level indicated the adduct

Table 3
Geometries at the HF/6-31G* and MP2/6-31G* levels ^{a)}

Species	Symmetry	HF/6-31G*	MP2/6-31G*
SiH ₄	T _d	$r_{\text{Si-H}} 1.475$, $\angle \text{HSiH} 109.47$	$r_{\text{Si-H}} 1.483$, $\angle \text{HSiH} 109.47$
H _a –H _b –Si–(H _c) ₃ [‡]	C _{3v}	$r_{\text{H}_a\text{-H}_b} 1.008$, $r_{\text{H}_b\text{-Si}} 1.708$, $r_{\text{Si-H}_c} 1.476$, $\angle \text{H}_b\text{SiH}_c 108.77$	$r_{\text{H}_a\text{-H}_b} 1.029$, $r_{\text{H}_b\text{-Si}} 1.670$, $r_{\text{Si-H}_c} 1.484$, $\angle \text{H}_b\text{SiH}_c 108.77$
H ₂	D _{∞h}	$r_{\text{H-H}} 0.730$	$r_{\text{H-H}} 0.737$
SiH ₃	C _{3v}	$r_{\text{Si-H}} 1.476$, $\angle \text{HSiH} 110.88$	$r_{\text{Si-H}} 1.483$, $\angle \text{HSiH} 111.25$

^{a)} Bond lengths in 10⁻¹⁰ m, and angles in deg.

Table 4
Frequencies at the HF/6-31G* and MP2/6-31G* levels ^{a)}

Species	HF/6-31G*	MP2/6-31G*
SiH ₄	907 (3), 939 (2), 2131 (3), 2138	909 (3), 955 (2), 2207, 2220 (3)
HSiH ₄	1842i, 318 (2), 846, 916 (2), 982, 1009 (2), 2120, 2129 (2)	1880i, 333 (2), 846, 926 (2), 1048 (2), 1057, 2192, 2216 (2)
H ₂	4154	4310
SiH ₃	781, 906 (2), 2111, 2128 (2)	765, 922 (2), 2186, 2222 (2)

^{a)} Vibrational frequencies in cm⁻¹, scaled by 0.893 at the HF/6-31G* level and 0.95 at the MP2/6-31G* level. Degeneracies are shown in parentheses.

to lie within ± 0.5 kJ mol⁻¹ of separated H + SiH₄, so this van der Waals complex is unlikely to be chemically significant.

Table 5 summarizes the components of the G2 calculation of the energy of the TS. The difference arising from the use of HF or MP2 ZPE is insignificant. Combination of our G2 result with literature G2 data for H and SiH₄ [42] yields E_0^\ddagger . Ab initio results for E_0^\ddagger and ΔH_0 , the enthalpy change for reaction (1) at 0 K, at different levels of theory are listed in table 6. We first compare calculated ΔH_0 values with experiment, because accuracy here is a prerequisite for reliable determination of E_0^\ddagger . The experimental ΔH_0 is derived from the measured $\Delta H_{f,298}(\text{SiH}_3)$ [51] together with $H_{298} - H_0(\text{SiH}_3)$ calculated by Hudgens [49], combined with similar tabulated information for the other species in reaction (1) [48]. The calculations at below the MP4/6-311G** level listed in

Table 5
Components of the G2 energy for the SiH₃[‡] transition state ^{a)}

Calculation	Energy
zero-point energy	0.02891 ^{b)}
MP4/6-311G**	-291.88923
PMP4/6-31G**	-291.89137
MP4/6-311+G**	-291.88961
MP4/6-311G**(2df)	-291.90980
QCISD(T)/6-311G**	-291.89289
MP2/6-311G**	-291.85631
MP2/6-311+G**	-291.85664
MP2/6-311G**(2df)	-291.87334
MP2/6-311+G(3df, 2p)	-291.87967

^{a)} At the MP2/6-31G* optimized geometry. Electronic energies are quoted in atomic units: 1 hartree \approx 2625 kJ mol⁻¹.

^{b)} Based on HF/6-31G* frequencies at the HF/6-31G* optimized geometry, scaled by 0.893.

Table 6
Enthalpies of the transition state and products relative to reactants at 0 K, E_0^\ddagger and ΔH_0 , for H + SiH₄ \rightarrow SiH₃[‡] \rightarrow H₂ + SiH₃

Calculation	E_0^\ddagger (kJ mol ⁻¹)	ΔH_0 (kJ mol ⁻¹)
HF/6-31G* ^{a)}	66.6	-25.2
MP2/6-31G* ^{b)}	54.8	-34.4
MP4/6-31G* ^{a)}	46.0	-44.8
MP4/6-31G* ^{b)}	47.7	-44.7
MP4/6-311G** ^{b)}	29.1	-50.7
G1 ^{c)}	23.9	-51.0
G2 ^{c)}	20.7	-54.7
G2* ^{b)}	21.2	-54.3
P-G2 ^{c)}	15.1	-55.5
expt. (see text)	17.1 \pm 3.0	-54.0 \pm 2.5

^{a)} At the HF/6-31G* optimized geometry, including scaled zero-point energy (ZPE) at the HF/6-31G* level.

^{b)} At the MP2/6-31G* optimized geometry, including scaled ZPE at the MP2/6-31G* level.

^{c)} At the MP2/6-31G* optimized geometry, including scaled ZPE at the HF/6-31G* level.

table 6 lead to ΔH_0 values which are significantly too positive. The recently revised experimental $\Delta H_{f,298}(\text{SiH}_3)$ significantly improves the agreement with the CISD + SCC/6-31G**||HF/6-31G* estimate of Tachibana et al., $\Delta H_0 = -59.4$ kJ mol⁻¹ [22]. The MP3/6-31G** calculations of Gordon et al. [21] and Tachibana et al. [22] yielded $\Delta H_0 = -52.3$ and -55.2 kJ mol⁻¹, respectively, both close to experiment, as is the MP4/6-311G(df, p) value of -54.4 kJ mol⁻¹ derived by Tachibana et al. from data of Pople et al. [52]. However the POL-CI/6-31G* value of -41.4 kJ mol⁻¹ by Gordon et al. is too positive [21].

Our G2 E_0^\ddagger value of about 21 kJ mol⁻¹ (see table 6) is the highest-level ab initio estimate to date, and suggests previous theoretical estimates are signifi-

cantly too positive. For example, Gordon et al. derived POL-CI/6-31G* and MP3/6-31G** values of 38.9 and 45.2 kJ mol⁻¹, respectively [21], and Tachibana et al. obtained MP3/6-31G** and CISD+SCC/6-31G** values of 39.7 and 32.2 kJ mol⁻¹, respectively [22]. Our new E_0^\ddagger is slightly larger than the experimental E_a but the difference is within the 8 kJ mol⁻¹ target accuracy of the G2 method [41]^{#2}, although of course E_0^\ddagger is *not the same* as E_a [20].

We have carried out kinetic modeling using TST, as outlined in section 2.2, to compare the theoretical and experimental kinetics, and to investigate the effects of tunneling. Eq. (3) was fitted to the experimental line of eq. (5) over 290–660 K with E_0^\ddagger as the only adjustable parameter. In the absence of a tunneling correction ($\Gamma=1$, model A) the best-fit TST result is $E_0^\ddagger = 14.6$ mol⁻¹, which fits the experimental data with a root-mean-square deviation of about 15% from eq. (5). A parameterization of the model A results over the range 290–2000 K is given in table 7. Model B applies the Wigner tunneling correction (eq. (4)) based on the ab initio $\nu^* = 1880$ cm⁻¹ from table 4. This model gives a close fit to the experimental results, with a root-mean-square deviation of 8% from eq. (5) over the experimental temperature range with $E_0^\ddagger = 18.1$ kJ mol⁻¹, and a parameterization is given in table 7. This value of ν^* is calculated at the MP2/6-31G* level of theory, but consideration of the E_0^\ddagger and ΔH_0 energies (table 6) shows that energy changes along the RC are poorly described at this

level. In particular, the barrier is too high, which will lead to an overestimate of the curvature i.e. ν^* and thus the tunneling correction. It would be desirable to employ frequencies calculated at a level of theory which correctly reproduces the energy changes along the RC, but a G2 frequency calculation is prohibitively expensive. Instead, we note that the geometry of the SiH₃ moiety is essentially unchanged during the course of reaction (along the MP2/6-31G* RC the Si–H bond lengths are constant to within 0.001 Å, while the HSiH bond angle is constant to within 2°), and thus the TS can be treated approximately as a linear triatomic molecule H–H–(SiH₃). G2 energies were obtained for two points on either side of the TS along the RC, for two different pairs of $r(\text{H–H})$ and $r(\text{H–Si})$. These data yield H–H and H–Si stretching force constants, on the assumption of a valence force model, which were employed as outlined by Herzberg [53] to derive an antisymmetric stretching frequency for the TS of $\nu^* = 1463$ cm⁻¹. This frequency leads to the model C results summarized in table 7, that also closely fit eq. (5), with a root-mean-square deviation of about 9% when $E_0^\ddagger = 17.1$ kJ mol⁻¹. Clearly, models A, B and C all fit experiment well; we prefer model C as it is the most physically realistic, and recommend it for extrapolation to temperatures above those investigated experimentally. A reasonable estimate of the uncertainty in E_0^\ddagger is about ± 3 kJ mol⁻¹, to allow for the dependence of E_0^\ddagger on the tunneling model selected. Fig. 3 shows a comparison of model C with experiment (the lines for models A and B lie too close to that for C to show separately), and the excellent accord supports the preexponential factor measured here over the smaller value obtained earlier [14]. The corresponding value of E_0^\ddagger is very close to the ab initio P-G2 estimate of 15.1 kJ mol⁻¹, and thus the kinetics can be rationalized in terms of a direct abstraction mechanism with no significant role for bound SiH₃ intermediates.

As a further test, we have estimated the kinetic isotope effect for reaction (1), defined here as $x = k(\text{H} + \text{SiH}_4)/k(\text{H} + \text{SiD}_4)$, and plot the results on fig. 4. Also shown there (by the solid curve) are data derived from the experimental results of Arthur et al. [14]. Agreement with the purely TST model A is only fair, and becomes worse if tunneling is included. A qualitatively similar discrepancy was seen in the case

^{#2} It should be noted that Pople and co-workers have *not* parameterized nor recommended their G2 method for transition states.

Table 7

Summary of transition state theory fits to experimental rate constants for H + SiH₄ in the form $k = A(T/K)^n \exp(-BK/T)$ cm³ s⁻¹

TST model (see text)	A	n	B
A ^{a)}	1.07×10^{-15}	1.736	1289
B ^{b)}	4.22×10^{-16}	1.829	1141
C ^{c)}	2.44×10^{-16}	1.903	1102

^{a)} No tunneling.

^{b)} Includes Wigner tunneling based on MP2/6-31G* value of ν^* .

^{c)} Includes Wigner tunneling based on a value of ν^* obtained from fitting to the G2 reaction coordinate.

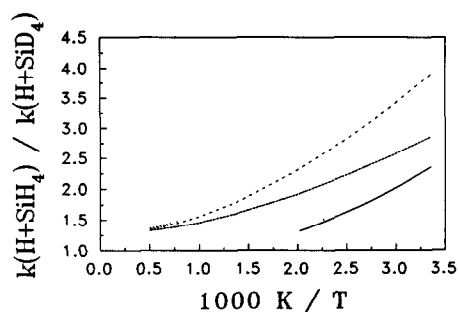


Fig. 4. Kinetic isotope effect for $\text{H} + \text{SiH}_4$: (—) experimental results from Arthur et al. [14]; (---) TST with no tunneling (model A); (···) TST with Wigner tunneling, ν^* from MP2/6-31G* theory (model B); (-·-·-) TST with Wigner tunneling, ν^* from G2 reaction coordinate (model C).

of $\text{O} + \text{SiH}_4$, where it was noted that reduction of the three highest frequency vibrations of the TS for that reaction by $\approx 200 \text{ cm}^{-1}$ each would lead to agreement [50]. However, it would also be worthwhile to verify the experimental kinetic isotope effect for reaction (1) by an alternative method.

4. Conclusions

The kinetics of the reaction $\text{H} + \text{SiH}_4$ have been measured from 290 to 660 K. The room-temperature results are in accord with several previous measurements. The higher-temperature results resolve a discrepancy concerning the preexponential factor, and are in excellent accord with TST calculations based on new ab initio results and a Wigner tunneling correction. The barrier height derived with G2 theory, when combined with a correction for spin contamination, is within 2 kJ mol^{-1} of the value obtained by fitting TST to the results. No theoretical evidence was found for bound SiH_3 intermediates, and such intermediates are not necessary to explain the kinetics.

Acknowledgement

We thank Dr. J.W. Hudgens of NIST for communicating unpublished thermodynamic data for SiH_3 . This work was supported by Texas Instruments, Inc., the Robert A. Welch Foundation (Grant B-1174) and the UNT Organized Research Fund.

References

- [1] M.J. Kushner, *J. Appl. Phys.* 62 (1987) 2803.
- [2] M.J. Kushner, *J. Appl. Phys.* 63 (1988) 2532.
- [3] K.J. Ryan and I.C. Plumb, *CRC Crit. Rev. Solid State Mater. Sci.* 15 (1988) 153.
- [4] A. Roth and F.J. Comes, *Ber. Bunsenges. Physik. Chem.* 95 (1991) 1296.
- [5] H. Niki and G.J. Mains, *J. Phys. Chem.* 68 (1964) 304.
- [6] P.D. Lightfoot and M.J. Pilling, *J. Phys. Chem.* 91 (1987) 3373.
- [7] G.K. Moortgat, Ph.D. Thesis, University of Detroit (1970).
- [8] J.-H. Hong, Ph.D. Thesis, University of Detroit (1972).
- [9] J.A. Cowfer, K.P. Lynch and J.V. Michael, *J. Phys. Chem.* 79 (1975) 1139.
- [10] K.Y. Choo, P.P. Gaspar and A.P. Wolf, *J. Phys. Chem.* 79 (1975) 1752.
- [11] E.A. Austin and F.W. Lampe, *J. Phys. Chem.* 81 (1977) 1134.
- [12] D. Mihelcic, V. Schubert, R.N. Schindler and P. Potzinger, *J. Phys. Chem.* 81 (1977) 1543.
- [13] K. Wörsdorfer, B. Reimann and P. Potzinger, *Z. Naturforsch.* 38a (1983) 896.
- [14] N.L. Arthur, P. Potzinger, B. Reimann and H.P. Steenbergen, *J. Chem. Soc. Faraday Trans. II* 85 (1989) 1447.
- [15] M. Koshi, F. Tamura and H. Matsui, *Chem. Phys. Letters* 173 (1990) 235.
- [16] B. Katz, J. Park, S. Satyapal, S. Tasaki, A. Chattopadhyay, W. Yi and R. Bersohn, *Faraday Discussions Chem. Soc.* 91 (1991) 73.
- [17] P. Potzinger, L.C. Glasgow and B. Reimann, *Z. Naturforsch.* 29a (1974) 493.
- [18] D. Mihelcic, P. Potzinger and R.N. Schindler, *Ber. Bunsenges. Physik. Chem.* 80 (1976) 565.
- [19] P. Marshall and A. Fontijn, *J. Chem. Phys.* 85 (1986) 2637.
- [20] H.S. Johnston, *Gas phase reaction rate theory* (Ronald, New York, 1966).
- [21] M.S. Gordon, D.R. Gano and J.A. Boatz, *J. Am. Chem. Soc.* 105 (1983) 5771.
- [22] A. Tachibana, Y. Kurosaki, K. Yamaguchi and T. Yamabe, *J. Phys. Chem.* 95 (1991) 6849.
- [23] L.C. Glasgow, G. Olbrich and P. Potzinger, *Chem. Phys. Letters* 14 (1972) 466.
- [24] K. Nakamura, N. Masaki, S. Sato and K. Shimokoshi, *J. Chem. Phys.* 83 (1985) 4504.
- [25] A. Demolliens, O. Eisenstein, P.C. Hiberty, J.M. Lefour, G. Ohanessian, S.S. Shaik and F. Volatron, *J. Am. Chem. Soc.* 111 (1989) 5623.
- [26] F. Volatron, P. Maître and M. Péliissier, *Chem. Phys. Letters* 166 (1990) 49.
- [27] J. Moc, J.M. Rudziński and H. Tatajczak, *J. Mol. Struct. THEOCHEM* 228 (1991) 131.
- [28] G.C. Schatz and S.P. Walch, *J. Chem. Phys.* 72 (1980) 776.
- [29] H. Furue and P.D. Pacey, *J. Phys. Chem.* 94 (1990) 1419.
- [30] N. Cohen, *Intern. J. Chem. Kinetics* 23 (1991) 683.
- [31] L. Ding and P. Marshall, *J. Phys. Chem.* 96 (1992) 2197.

- [32] Y. Shi and P. Marshall, *J. Phys. Chem.* 95 (1991) 1654.
- [33] T. Ko, P. Marshall and A. Fontijn, *J. Phys. Chem.* 94 (1990) 1401.
- [34] J.A.R. Samson, *Techniques of vacuum ultraviolet spectroscopy* (Wiley, New York, 1967) p. 204.
- [35] L. Ding and P. Marshall, *J. Chem. Soc. Faraday Trans.* 89 (1993) 419.
- [36] W.J. Hehre, L. Radom, P. von R. Schleyer and J.A. Pople, *Ab initio molecular orbital theory* (Wiley, New York, 1986).
- [37] M.J. Frisch, M. Head-Gordon, G.W. Trucks, J.B. Foresman, H.B. Schlegel, K. Raghavachari, M.A. Robb, J.S. Binkley, C. Gonzalez, D.J. DeFrees, D.J. Fox, R.A. Whiteside, R. Seeger, C.F. Melius, J. Baker, R.L. Martin, L.R. Kahn, J.J.P. Stewart, S. Topiol and J.A. Pople, *GAUSSIAN 90* (Gaussian, Pittsburgh, 1990).
- [38] R. Seeger and J.A. Pople, *J. Chem. Phys.* 66 (1977) 3045.
- [39] C. Gonzales and H.B. Schlegel, *J. Chem. Phys.* 90 (1989) 2154.
- [40] J.A. Pople, M. Head-Gordon, D.J. Fox, K. Raghavachari and L.A. Curtiss, *J. Chem. Phys.* 90 (1989) 5622.
- [41] L.A. Curtiss, C. Jones, G.W. Trucks, K. Raghavachari and J.A. Pople, *J. Chem. Phys.* 93 (1990) 2537.
- [42] L.A. Curtiss, K. Raghavachari, G.W. Trucks and J.A. Pople, *J. Chem. Phys.* 94 (1991) 7221.
- [43] H.B. Schlegel, *J. Chem. Phys.* 84 (1986) 4530.
- [44] M.F.R. Mulcahy, *Gas kinetics* (Nelson, London, 1973).
- [45] J.A. Irvin and T.I. Quickenden, *J. Chem. Educ.* 60 (1983) 711.
- [46] K. Héberger, S. Kemény and T. Vidóczy, *Intern. J. Chem. Kinetics* 19 (1987) 171.
- [47] M.E. Coltrin, R.J. Kee and J.A. Miller, *J. Electrochem. Soc.* 133 (1986) 1206.
- [48] M.W. Chase Jr., C.A. Davies, J.R. Downey Jr., D.J. Frurip, R.A. McDonald and A.N. Syverud, *JANAF thermochemical tables*, 3rd Ed.; *J. Phys. Chem. Ref. Data* 14 (1985) Suppl. No. 1.
- [49] J.W. Hudgens, private communication, January 1992.
- [50] L. Ding and P. Marshall, *J. Chem. Phys.* 98 (1993) 8545.
- [51] J.A. Seetula, Y. Feng, D. Gutman, P.W. Seakins and M.J. Pilling, *J. Phys. Chem.* 95 (1991) 1658.
- [52] J.A. Pople, B.T. Luke, M.J. Frisch and J.S. Binkley, *J. Chem. Phys.* 89 (1985) 2198.
- [53] G. Herzberg, *Molecular spectra and molecular structure*, Vol. 2. *Infrared and Raman spectra of polyatomic molecules* (Van Nostrand, New York, 1945) ch. 4.